Surface Chemistry of Boron Oxidation. 2. The Reactions of B_2O_2 and B_2O_3 with Boron Films Grown on Ta(110)

Yajun Wang and Michael Trenary*

Department of Chemistry, M/C 111, University of Illinois at Chicago, Chicago, Illinois 60680

Received August 26, 1992. Revised Manuscript Received November 23, 1992

We have used X-ray photoelectron spectroscopy (XPS) and temperature-programmed desorption (TPD) to study the reactions of B_2O_2 and isotopically pure $^{10}B_2O_3$ with boron thin films grown on the Ta(110) surface. The B_2O_2 and $^{10}B_2O_3$ were directly deposited on the boron film from a Knudsen cell. XPS spectra show that B_2O_2 disproportionates to B_2O_3 and boron at temperatures of 600–800 K. TPD experiments show that surface oxide desorption takes place at temperatures of 1100–1250 K and that the dominant desorbing species is $B_2O_2(g)$ regardless of whether B_2O_3 or B_2O_2 is initially deposited. When isotopically pure $^{10}B_2O_3$ reacts with the boron film containing the natural abundance ^{11}B:^{10}B ratio of 4:1, the desorbing B_2O_2 also displays a ^{11}B:^{10}B ratio of nearly 4:1. This indicates almost complete exchange of boron atoms between the oxide layer and the boron substrate.

Introduction

In several previous publications[1-4] we have discussed the importance of the oxidation of solid elemental boron and have presented experimental results for the reactions of O_2 and B_2O_3 with boron surfaces. The first studies were of the (111) surface of a single crystal of β-rhombohedral boron,[1-3] and in the first paper[4] of this two-paper series we presented results for boron thin films grown from the thermal decomposition of diborane on the Ta(110) surface. In these previous studies we have found that at least two boron oxides, B_2O_3 and B_2O_2, play a significant role in the reaction of O_2 with boron. More specifically, for the B/Ta(110) system X-ray photoelectron spectroscopy (XPS) shows that a submonolayer of B_2O_3 forms on the boron surface while temperature-programmed desorption (TPD) results show that the oxide that forms from the reaction of O_2 with the surface desorbs manily as B_2O_2.

The fact that more than one boron oxide is involved in the oxidation chemistry of boron is not surprising when one considers that a variety of boron–oxygen compounds,[5-16] in addition to B_2O_3, are known. The B_2O_2 molecule has been well-characterized spectroscopically both in the gas phase and trapped in rare-gas matrixes.[8-13] It has the O=B—B=O structure. A $(BO)_x$ solid has been reported but not well-characterized.[6,7,9,14] The preparation and properties of a stable and extremely hard material with a B_6O stoichiometry have been described in detail.[15,16] Other boron oxides have also been reported.[5] If one considers not only neutral species but also borate anions which form salts with metal cations or hydrated borate anions found in solution, one finds that there are a rather large number of known species with the general B_nO_m stoichiometry.[17] The present study is concerned only with the interactions of B_2O_3 and B_2O_2 with boron surfaces because they are the only two boron oxides that have already been shown to play a role in boron oxidation.

Experimental Section

The apparatus used in these studies has been described in detail elsewhere.[1-4] Briefly, the experiments were conducted in an ultrahigh-vacuum (UHV) chamber (base pressure $\leq 1 \times 10^{-10}$ Torr) equipped with low-energy electron diffraction (LEED) optics, an X-ray photoelectron spectroscopy (XPS) system, and a quadrupole mass spectrometer for residual gas analysis and temperature-programmed desorption (TPD) experiments.

The XPS system consists of a hemispherical electron energy analyzer (CLAM 100, VG Microtech) and a dual Mg/Al anode X-ray source (VG Microtech). The XPS binding energies were calibrated with a piece of silver foil, cleaned with Ar^+ ion sputtering, mounted above the sample. Using Mg Kα radiation and a constant analyzer pass energy of 20 eV which yields a nominal resolution of 1.0 ev, the silver foil gave a binding energy of 368.35 eV and a line width (fwhm) of 0.988 eV for the Ag($3d_{5/2}$) transition. This binding energy is within 0.1 eV of the calibration value of 368.29 ± 0.01 eV published by Anthony.[18] All XPS spectra were obtained using the Al anode (Al Kα radiation, 1486.6 eV) at a power of 600 W (15 kV, 40-mA emission current) with a constant analyzer pass energy of 50 eV corresponding to a nominal resolution of 1.8 eV.

The preparation and cleaning of the Ta(110) surface and the growth and characterization of the B films are described in detail

* To whom correspondence should be addressed.

(1) Foo, W. C.; Ozcomert, J. S.; Trenary, M. *Surf. Sci.* **1991**, *255*, 245.
(2) Foo, W. C.; Ozcomert, J. S.; Trenary, M. *Surf. Sci.* **1992**, *262*, 88.
(3) Foo, W. C. Ph.D. Dissertation, The University of Illinois at Chicago, 1991.
(4) Wang, Y.; Trenary, M., *Chem. Mater.*, previous article in this issue.
(5) Galchenko, G. L.; Lavut, E. G.; Lavut, E. A.; Vidavsky, L. M. In *Boron and Refractory Borides*; Matkovich, V. I., Ed.; Springer-Verlag: Berlin, 1977.
(6) Wartik, T.; Apple, E. F. *J. Am. Chem. Soc.* **1955**, *77*, 6400.
(7) McCloskey, A. L.; Brotherton, R. J.; Boone, J. L. *J. Am. Chem. Soc.* **1961**, *83*, 4750.
(8) Sheer, M. D. *J. Phys. Chem.* **1958**, *62*, 490.
(9) Kanda, F. A.; King, A. J.; Russell, V. A.; Katz, W. *J. Am. Chem. Soc.* **1956**, *78*, 1509.
(10) Weltner, Jr., W.; Warn, J. R. W. *J. Chem. Phys.* **1962**, *37*, 292.
(11) Sommer, A.; White, D.; Linevsky, M. J.; Mann, D. E. *J. Chem. Phys.* **1963**, *38*, 87.
(12) Ruščić, B. M.; Curtiss, L. A.; Berkowitz, J. *J. Chem. Phys.* **1984**, *80*, 3962.
(13) Inghram, M. G.; Porter, R. F.; Chupka, W. A. *J. Chem. Phys.* **1956**, *25*, 498.
(14) Nicholls, D. *J. Chem. Soc.* **1965**, 6644.
(15) Rizzo, H. F.; Simmons, W. C.; Bielstein, H. O. *J. Electrochem. Soc.* **1962**, *78*, 1079.
(16) Petrak, D. R.; Ruh, R.; Goosey, B. F. NBS Special Pubications No. 364; National Bureau of Standards: Washington, 1972; pp 605–611.
(17) Cotton, F. A.; Wilkinson, G. *Advanced Inorganic Chemistry*, 5th ed.; Wiley: New York, 1988; Chapter 6.
(18) Anthony, M. T. In *Practical Surface Analysis by Auger and X-ray Photoelectron Spectroscopy*; Briggs, D., Seah, M. P., Eds.; Wiley: New York, 1983.

0897-4756/93/2805-0199$04.00/0

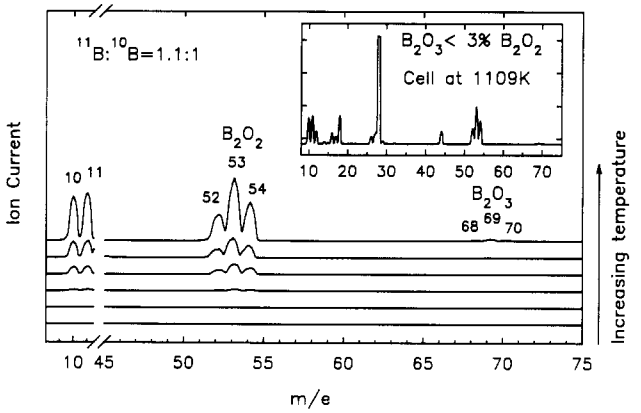

Figure 1. Mass spectra of the gas effusing from our $B_2O_2(g)$ source as a function of temperature. An isotopic ratio of $^{11}B:^{10}B$ = 1.1:1 was obtained from these spectra. At 1109 K, the amount of $B_2O_3(g)$ is less than 3% of the amount of $B_2O_2(g)$.

in the first paper of the present two-paper series.[4] There we show that clean boron films at least 3 nm thick can be deposited on the Ta(110) surface through the thermal decomposition of $B_2H_6(g)$ at temperatures of 600–750 K. The $B_2H_6(g)$ and hence the boron films had the natural abundance ratio of $^{11}B:^{10}B$ of 4:1. When these boron films are annealed to temperatures above 1100 K they react with the substrate to form a TaB_2 layer. After the first formation of the TaB_2 layer, heating of subsequently deposited boron films to temperatures higher than 1100 K appears to lead to the growth of a thicker TaB_2 layer rather than the development of crystalline forms of boron. Attempts to observe LEED patterns of the boron films were unsuccessful which is consistent with an amorphous structure as expected from the low temperature of the deposition.

The design and characterization of the source used for the direct deposition of B_2O_3 has been given in detail elsewhere.[2,3] The cell used for B_2O_2 deposition is similar in design. A brief description of each source follows. The B_2O_3 and B_2O_2 sources consist of cylindrical molybdenum crucibles 1 cm in diameter and 1 cm in height with removable tops. Source temperature is measured with a chromel–alumel thermocouple spot-welded to the side of the crucible near a 3-mm diameter hole for effusion of the $B_2O_3(g)$ or $B_2O_2(g)$. Coils of Mo wire inside the crucibles serve as resistive heaters. The B_2O_3 is made by heating boric acid through the reaction $2B(OH)_3 \rightarrow B_2O_3 + 3H_2O$. The loss of water is complete before the melting point of B_2O_3 at 723 K. Mass spectra of the isotopically enriched (99.2% ^{10}B) boric acid (Eagle-Picher, Inc.) gave a $^{10}B_2O_3^+$ (m/e = 68) to $^{10}B^{11}BO_3^+$ (m/e = 69) ratio consistent with the quoted isotopic purity. The B_2O_3 source showed a parent ion ($^{10}B_2O_3$ at m/e = 68) to $^{10}B_2O_2$ fragment ion (at m/e = 52) ratio of 13:1. This value is somewhat higher than we reported earlier.[3] It is difficult to establish whether some B_2O_2 effuses from the B_2O_3 source or if the m/e = 52 peak is due entirely to B_2O_3 fragmentation. The higher (m/e = 68)/(m/e = 52) ratio observed here suggests that some B_2O_2 effuses from the source and that the amount can vary.

The method for producing B_2O_2 is similar to that used by others[8-14] and is based on the reaction $2B + 2B_2O_3(l) \rightarrow 3B_2O_2(g)$. Although isotopically pure $^{10}B_2O_2(g)$ would be produced from isotopically pure ^{10}B and $^{10}B_2O_3$, we found that it was difficult to achieve complete reaction with crystalline boron powder which was the only form of ^{10}B available. Good results were achieved with amorphous boron powder (Johnson Matthey Electronics) which had the natural abundance composition of 80.2% ^{11}B and 19.8% ^{10}B. This boron and isotopically enriched $^{10}B_2O_3$ were used at a molar ratio of ≈1.5:1 to ensure complete reaction. Figure 1 shows mass spectra from the $B_2O_2(g)$ source at several temperatures. An isotopic ratio of $^{11}B:^{10}B$ = 1.1:1 was obtained. The following fragment ions were observed: $^{10}B^+$ (m/e = 10), $^{11}B^+$ (m/e = 11), $^{10}BO^+$ (m/e = 26), and $^{11}BO^+$ (m/e = 27). The mass spectrum at 1109 K shows that the amount of $B_2O_3(g)$ is less than 3% of the amount of $B_2O_2(g)$. This is a lower ratio than reported earlier by Inghram and co-workers[13] for a source temperature of 1500 K. A stainless steel flag attached to a linear motion feedthrough was placed directly in front of the source opening. Precise exposures were achieved by pulling back the flag for the desired amount of time.

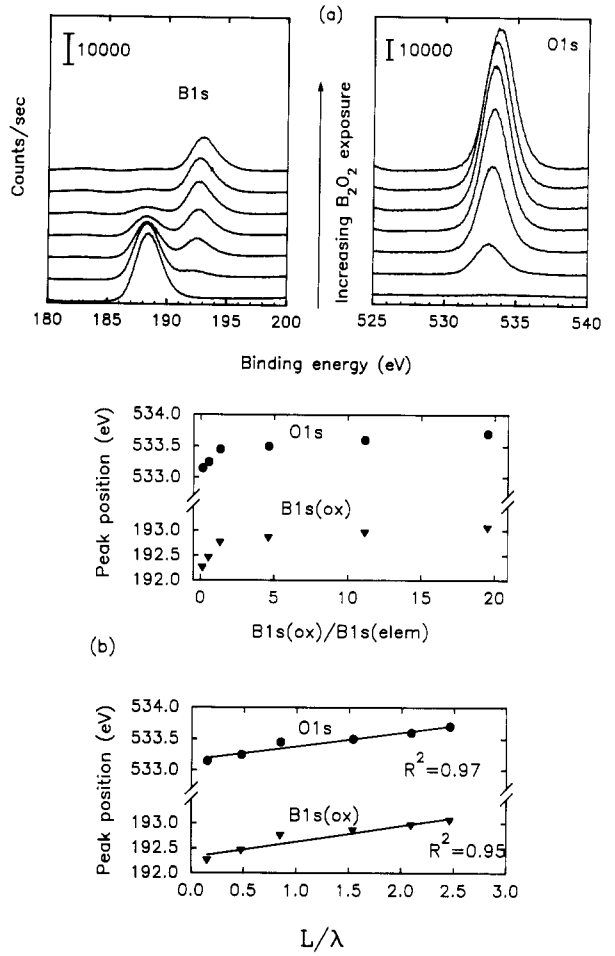

Figure 2. (a) XPS spectra of the B(1s) and O(1s) regions as a function of $B_2O_2(g)$ exposure. (b) Plot of the O(1s) and B(1s) binding energies as a function of the B(1s) (ox)/B(1s) (elem) ratio and as a function of B_2O_2 layer thickness, L, divided by λ, the mean free path of the photoelectrons in the film.

Results

We have characterized B_2O_2 and B_2O_3 deposited on the surface of the boron film with XPS. While solid B_2O_3 has been well-characterized with XPS in the past both by our group[2,3] and by others,[19] we have recently obtained what appears to be the first XPS spectra of condensed B_2O_2. The B_2O_2 XPS results are reported here and with complete instrumental specifications elsewhere.[20] We find that the B(1s) chemical shift is sufficiently different in B_2O_3 and B_2O_2 to allow the two oxides to be unambiguously distinguished. However, to do so requires careful consideration of the dependence of the binding energy on the thickness of the oxide layer. We assume that $B_2O_2(s)$, like $B_2O_3(s)$, is an insulator although we do not know of any measurements of the electrical properties of $B_2O_2(s)$.

Figure 2a shows the B(1s) and O(1s) regions as a function of increasing B_2O_2 exposure times with the source held at a temperature of 1085 K. The B_2O_2 yields a shifted B(1s) peak in the range of 192.0–193.0 eV in addition to an O(1s) peak in the range of 533.0–534.0 eV. The two B(1s) peaks

(19) Joyner, D. J.; Hercules, D. M. *J. Chem. Phys.* **1980**, *72*, 1095.
(20) Wang, Y.; Trenary, M. *Surf. Sci. Spectra*, in press.

can be fit with two Gaussian functions using a linear background substraction. This permits B(1s) peak areas for the elemental boron, B(1s) (elem), and for the oxidized boron, B(1s) (ox), to be obtained. The ratio of the O(1s) peak area to the B(1s) (ox) peak area from six B_2O_2 spectra is 6.1 ± 0.2. This ratio agrees with the reported O(1s)/B(1s) XPS sensitivity factor ratios of 6.0[21] and 6.7 ± 0.9.[1-3] We observe a shift to higher binding energies for the B(1s) and O(1s) peaks with increasing B_2O_2 exposure times.

The exact functional dependence of binding energy on layer thickness is established by the plots of Figure 2b. The upper plot shows the O(1s) and B(1s) (ox) peak positions as a function of the B(1s) (ox)/B(1s) (elem) peak area ratio. The B(1s) (ox) and the O(1s) peaks undergo shifts of about 0.8 eV although the difference in their binding energies remains constant at 340.8 ± 0.1 eV. Although the B(1s) (ox)/B(1s) (elem) peak area ratio is related to the thickness of the oxide layer, it would be better to plot the binding energies against a quantity directly proportional to layer thickness. By assuming that the mean free paths, λ, of the B(1s) electrons of the oxidized and unoxidized boron are the same, the normalized peak area ratio, R, is related to the layer thickness, L, by[22]

$$R = \exp(L/\lambda \cos\theta) - 1$$

where θ is the electron detection angle measured from the surface normal which was 47° for these experiments. The B(1s) peak areas need to be normalized to their values for the clean boron film, I°(elem), and for a very thick oxide layer, I°(ox). The latter quantity is obtained for an oxide layer thick enough that the B(1s) (elem) peak is not visible. The normalization adjusts for factors such as the different number densities of boron atoms in the pure boron film and in the oxide. From the normalized ratios, R, we calculate (cos θ) ln [R + 1] = L/λ and plot the binding energies versus L/λ in the lower plot. Although the exact value of λ is unknown, it has been estimated[24] to be 22 Å for boron. From the measured ratios, Figure 2b indicates that the peak position depends linearly on L/λ.

The same method can be applied to the deposition of B_2O_3 on the boron film. Figure 3a shows the B(1s) and O(1s) regions as a function of increasing exposure times to the B_2O_3 source held at a temperature of 1150–1153 K. The B_2O_3 gives rise to a shifted boron peak in the range of 193.5–194.5 eV in addition to the O(1s) peak in the range of 533.5–534.5 eV. The difference in the binding energy between O(1s) and B(1s) (ox) is constant at 339.7 ± 0.1 eV. A value of 9.1 ± 0.5 was obtained for the O(1s)/B(1s) (ox) peak area ratio from six spectra of B_2O_3 on the boron film. A linear dependence for the peak position on layer thickness was also obtained for B_2O_3 as shown in Figure 3b.

There are two possibilities for the observed binding energy shifts. For nonconducting samples, it is well-known that the development of a surface charge shifts the measured binding energies and can broaden the peaks.[21,23] Others have reported a linear dependence of the charging

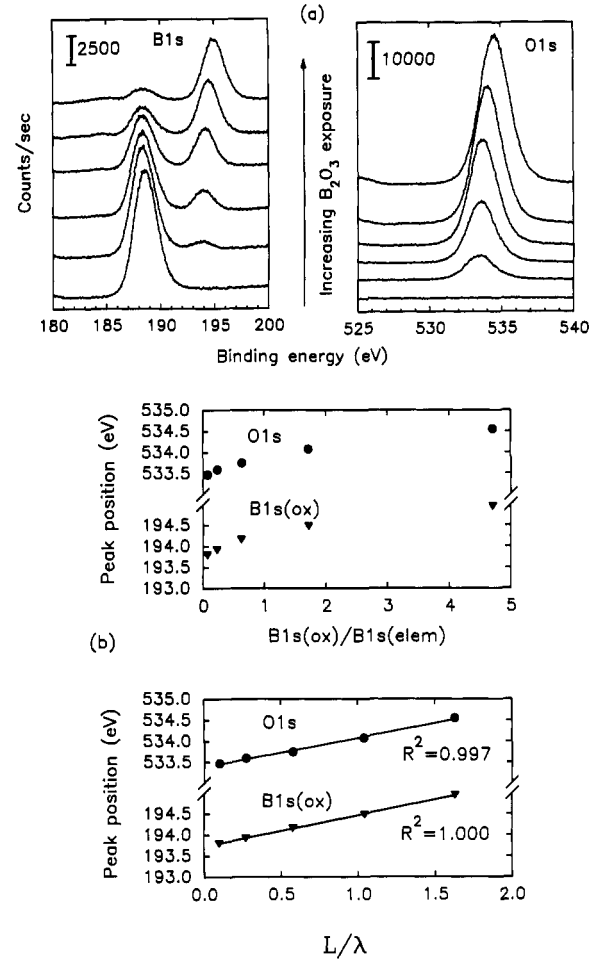

Figure 3. (a) XPS spectra of the B(1s) and O(1s) regions as a function of B_2O_3(g) exposure. The B_2O_3 source was held at 1153 K during the exposure. (b) Plot of the O(1s) and B(1s) binding energies as a function of both the B(1s) (ox)/B(1s) (elem) ratio and as a function of B_2O_3 layer thickness, L, divided by λ, the mean free path of the photoelectrons in the film.

shift on layer thickness.[25] However, a linear dependence was also observed for oxide layers on Si surfaces where charging effects were ruled out.[26] Instead, extraatomic relaxation of the final state in the oxide was suggested. Further experiments are needed to identify the origin of the shifts in Figures 2 and 3. However, for the purposes of this paper, Figures 2 and 3 serve to empirically establish the XPS features which distinguish the two boron oxides: a B(1s) binding energy of 192.0–193.0 eV and an O(1s)/B(1s) (ox) ratio of 6.1 is characteristic of B_2O_2 while a binding energy of 193.5–194.5 eV and a O(1s)/B(1s) (ox) peak area ratio of 9.1 serves to identify B_2O_3.

During the direct deposition of B_2O_2 and B_2O_3, the substrate boron films were kept at room temperature. Figure 4a shows XPS spectra of the B(1s) and O(1s) regions as a function of annealing temperature after an initial B_2O_3 deposition at room temperature. All spectra were taken after the heating current was turned off and after the sample had cooled to 300–350 K. Figure 4b shows plots of the O(1s) peak area, the O(1s)/B(1s) (ox) peak area ratio, and the B(1s) (ox) binding energy as a function of annealing temperature. The intensity of the O(1s) peak begins to drop after the sample has been heated to 1000

(21) *Handbook of X-ray Photoelectron Spectroscopy*; Muilenburg, G. E., Ed.; Perkin-Elmer: Eden Prairie, MN, 1979.
(22) Hofmann, S. In *Practical Surface Analysis by Auger and X-ray Photoelectron Spectroscopy*; Briggs, D., Seah, M. P., Eds.; Wiley: New York, 1983.
(23) Briggs, D.; Seah, M. P. *Practical Surface Analysis by Auger and X-ray Photoelectron Spectroscopy*; Wiley: New York, 1983.
(24) Penn, D. R. *J. Electron Spectrosc. Relat. Phenom.* **1976**, *9*, 29.
(25) Clark, D. T.; Dilks, A.; Thomas, H. R.; Shuttleworth, D. *J. Polym. Sci., Polym. Chem. Ed.* **1979**, *17*, 627.
(26) Finster, J.; Schulze, D. *Phys. Status Solidii* **1981**, *68*, 505.

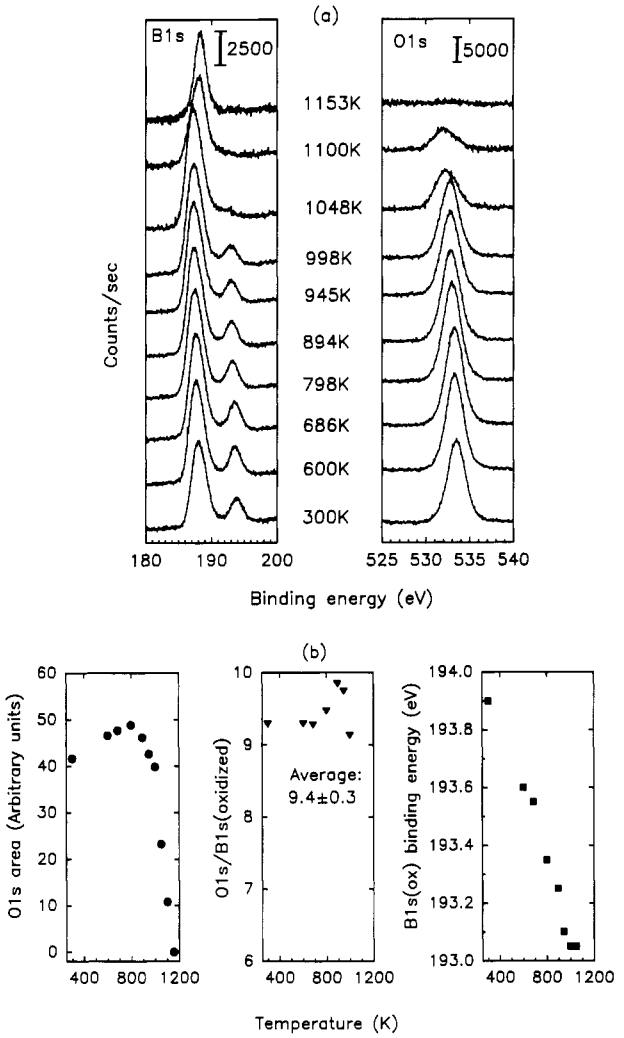

Figure 4. (a) XPS spectra of the B(1s) and O(1s) regions taken at room temperature as a function of annealing temperature after initial B_2O_3 deposition from the source held at 1083 K. (b) Plot of the O(1s) peak area, B(1s) binding energy, and O(1s)/B(1s) (ox) peak area ratio as a function of annealing temperature. The plots were prepared from the spectra of (a).

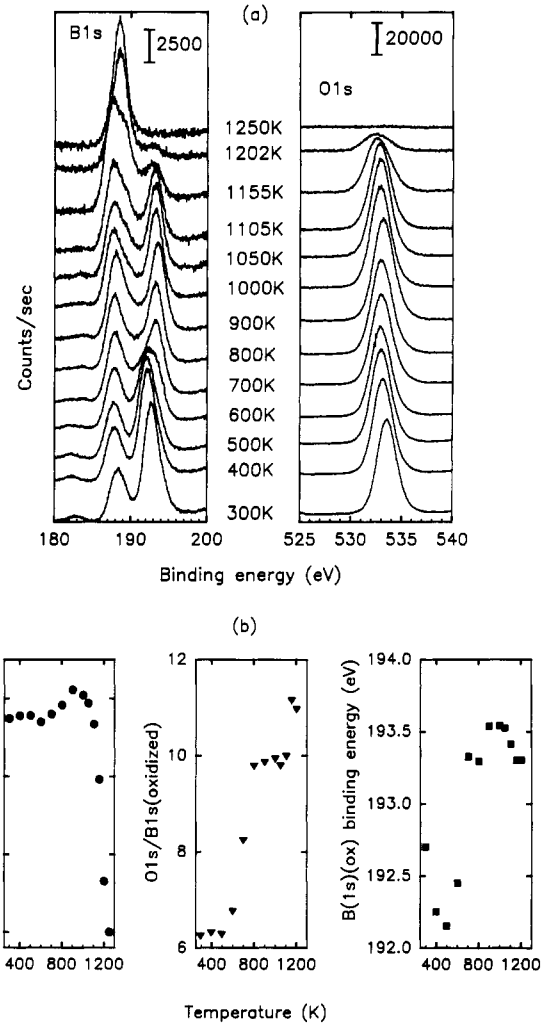

Figure 5. (a) XPS spectra of the B(1s) and O(1s) regions taken at room temperature as a function of annealing temperature after initial B_2O_2 deposition from the source held at 1083 K. (b) Plot of the O(1s) peak area, B(1s) binding energy, and O(1s)/B(1s) (ox) peak area ratio as a function of annealing temperature. The plots were prepared from the spectra of (a).

K, then totally disappears after 1150 K. This indicates that the desorption of oxygen-containing species takes place in the temperature range 1000–1200 K. As shown in Figure 4b the O(1s)/B(1s) (ox) peak area ratios fall in the range 9.0–10.0 with an average of 9.4 ± 0.3, a characteristic of the B_2O_3 stoichiometry. The B(1s) binding energy is higher than 193.1 eV for all annealing temperatures even as its intensity becomes much smaller. This indicates that the deposited oxide retains the characteristics of B_2O_3 up to the oxide desorption temperature.

Figure 5 shows results for B_2O_2 deposited on the surface of a boron film which are analogous to the B_2O_3 results of Figure 4. The intensity of the O(1s) peak begins to drop only after the sample has been heated to 1050 K and then totally disappears after 1250 K. It indicates that the desorption of oxygen-containing species takes place in the temperature range 1050–1250 K. As the temperatures increase, not only does the intensity of the B(1s) (ox) peak change but its position and shape also change. The B(1s) region was fit to several Gaussian functions to obtain the B(1s) (ox) peak area. As shown in Figure 5b the O(1s)/B(1s) (ox) peak area ratio is 6.1 at room temperature, begins to increase at 600 K, and then reaches a constant value of 10 above 800 K. The O(1s)/B(1s) (ox) ratios above 1150 K show more scatter due to the low intensity of the peaks. The B(1s) (ox) binding energy starts at 192.7 eV for B_2O_2 and then changes to 193.5 eV after 800 K. From both the change in the B(1s) binding energy and in the O(1s)/B(1s) (ox) peak area ratio, it is clear that the initially deposited B_2O_2 has been transformed into B_2O_3 in the temperature range 600–800 K, well below the temperature of oxide desorption. The elemental B(1s) peak changes from a binding energy of 188.3 to 188.0 eV, finally shifting up to 189.0 eV for TaB_2. Similar changes were observed in the XPS spectra of B_2O_2 deposited on the surfaces of clean Ta(110) and of TaB_2/Ta(110). There is an initial decrease of the B(1s) binding energy of B_2O_2 from room temperature to 500 K which may be due to structural changes in the deposited B_2O_2, similar to changes reported in an XPS analysis of CoO.[27]

Several common features of both Figures 4 and 5 should be noted. There is a rise in the O(1s) intensity and a shift of the B(1s) peak to lower binding energies with increasing annealing temperature. These changes are most likely

(27) Rizzetti, A.; Xhie, J.; Sattler, K.; Yamamoto, D.; Pong, W. *J. Electron Spectrosc. Relat. Phenom.* **1992**, *58*, 359.

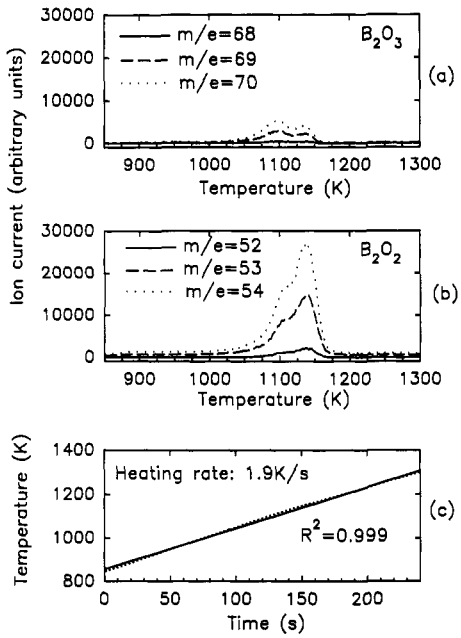

Figure 6. TPD results obtained simultaneously for the six possible B_2O_2 and B_2O_3 isotopes after an initial deposition of $^{10}B_2O_3$.

due to irreversible structural changes in the oxide layer which lead to an increase in density and consequently a decrease in thickness. A thinner layer will result in a smaller charging shift while a denser layer will result in an increase in the O(1s) and B(1s) (ox) peak areas. Changes in the structure of B_2O_3 with temperature have been recently studied with Raman spectroscopy.[28] We note that the spectra obtained following annealing temperatures above about 1050 K display higher noise levels particularly in the B(1s) region. This is most likely due to an increase in background electrons due to inelastically scattered electrons from the Ta(4f) peak. As described in the previous paper,[4] annealing the boron films to ≈1100 K results in the formation of TaB_2 and hence a reappearance of the Ta(4f) peak in the XPS spectrum.

Figure 6 shows TPD results for various possible B_2O_3 and B_2O_2 isotopes after depositing $^{10}B_2O_3$ on the boron film surface at room temperature. Figure 6c shows that the heating rate was linear over the region of oxide desorption. During the course of these experiments several other mass channels were monitored including m/e = 10 (^{10}B), m/e = 11 (^{11}B), m/e = 26 (^{10}BO), m/e = 27 (^{11}BO), m/e = 38 ($^{11}B_2O$), and m/e = 43 ($^{11}BO_2$). Neither B_2O nor BO_2 desorption was observed. The ^{10}B, ^{11}B, ^{10}BO, and ^{11}BO peaks occur at the same temperature as the B_2O_2 peak and occur in the same ratio to the B_2O_2 peak as in the mass spectrum of the B_2O_2 source. The identification of the m/e = 10, 11, 26, and 27 peaks as due to B and BO is confirmed by the isotope ratio of ^{11}B:^{10}B = 4:1 which is characteristic of all molecules containing boron with the natural abundance of ^{11}B and ^{10}B. The mass spectrum of pure B_2O_3 consists primarily of the parent ion with only a small B_2O_2 fragment indicating that the results of Figure 6 are not due to B_2O_3 desorption. The fact that B_2O_2 desorbs before 1200 K for this coverage is consistent with the XPS results of Figure 5b. We observe an isotopic ratio of $^{11}B_2O_2$:$^{11}B^{10}BO_2$:$^{10}B_2O_2$ of 15.0:7.5:1, which is

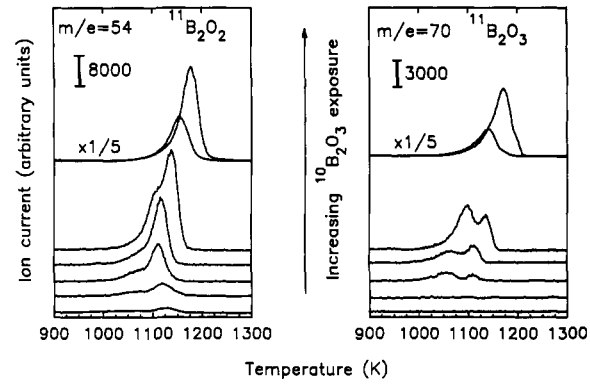

Figure 7. Variation of the $^{11}B_2O_2$ and $^{11}B_2O_3$ desorption peaks with initial $^{10}B_2O_3$ coverage.

almost identical to the natural abundance ratio of 16:8:1. This indicates that there has been extensive isotopic exchange between the deposited $^{10}B_2O_3$ and the boron film. We observed a similar complete isotopic exchange in experiments of $^{10}B_2O_3$ deposited on the surface of single crystal boron.[2,3] However, in the previous study an isotopically pure $^{10}B_2O_3$ peak was also observed at lower temperatures. As discussed below, the shape of the desorption peaks depends on initial B_2O_3 coverage.

Figure 7 shows the $^{11}B_2O_2$ (m/e = 54) and $^{11}B_2O_3$ (m/e = 70) thermal desorption peaks as a function of increasing B_2O_3 exposure. The B_2O_2 and B_2O_3 peak maxima are observed in the range 1000–1200 K. At the lowest two exposures we observe a B_2O_2 peak at 1125 K but no B_2O_3 peak. For the next two exposures we observe a main B_2O_2 peak at the same temperature of 1110 K for both exposures and a lower temperature shoulder. For these two exposures we see two B_2O_3 peaks at 1050 and 1105 K. After the third highest exposure, the main B_2O_2 peak has shifted to 1140 K and a distinct shoulder is visible at 1105 K. For this exposure, the B_2O_3 peaks have shifted to higher temperatures with the lower temperature peak now the larger of the two. For much higher exposures (note the different scale) the peaks shift to higher temperatures and display a more or less common leading edge. The fact that the leading edges are not exactly coincident is probably due to slight variations in the experimental conditions. Due to the long times needed to grow the boron films and the fact that a new film is needed for each TPD run, it was necessary to perform each experiment on a different day. Slight variations in mass spectrometer sensitivity, thermocouple response, resistive heating power supply, etc., could lead to the observed deviations from a common leading edge which we assume we would have observed under ideal conditions. A common leading edge and a shift in peak maxima to higher temperatures are characteristics of zero order desorption which indicates desorption of multilayers.

The XPS results of Figure 5 indicate that B_2O_2 disproportionates to B_2O_3 and B at temperatures above 800 K while no oxide desorption takes place until temperatures above 1000 K. This suggests that the same thermal desorption results should be obtained following B_2O_2 or B_2O_3 deposition. This expectation is confirmed by the results of Figure 8. As before, the main desorbing species is B_2O_2 with a smaller amount of B_2O_3 observed. The deposited B_2O_2 contained a ^{11}B:^{10}B ratio of 1.1:1.0 while the desorbing species had a ^{11}B:^{10}B ratio of 4.2:1.0, essentially the same as the natural abundance ratio. Figures 6 and 8 are clearly not identical. The B_2O_2 peak

(28) Hassan, A. K.; Torell, L. M.; Börjesson, L. *Phys. Rev. B* **1992**, *45*, 12797.

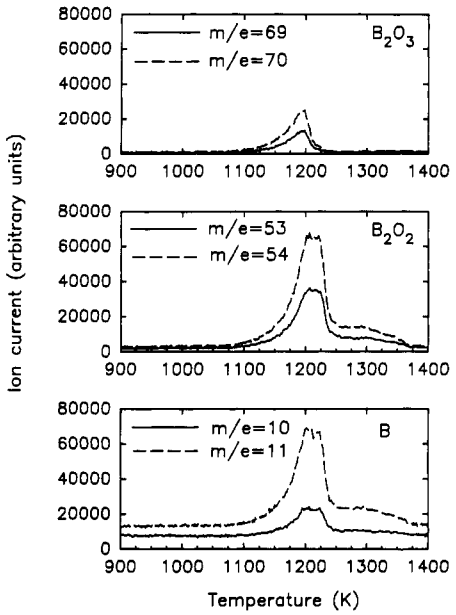

Figure 8. TPD results obtained simultaneously for the possible B_2O_2, B_2O_3, and ^{11}B, ^{10}B isotopes after an initial deposition of B_2O_2 with a ^{11}B:^{10}B ratio of 1.1:1.

has a flattened top in Figure 8 indicating unresolved structure and occurs at a temperature of 1200 K while in Figure 6 the B_2O_2 peak occurs in the range 1100–1150 K. However, as Figure 7 shows, the peak shapes and the temperature of the peak maxima change significantly with coverage. On the basis of the B_2O_2 intensity scales of Figures 7 and 8, we estimate that the B_2O_3 coverage in Figure 8 would imply a desorption peak between 1150 and 1175 K. Thus the 1200 K B_2O_2 peak temperature in Figure 8 cannot be attributed simply to a higher B_2O_3 coverage than in Figure 6. The difference may either be due to real physical differences in the system arising from differences in B_2O_3 and B_2O_2 deposition, or to inaccuracies in the temperature. We should note that the type C thermocouple used for Figures 6 and 7 was replaced with a second type C thermocouple for the experiments of Figure 8. Comparisons with pyrometer readings indicate that the thermocouple used for Figures 6 and 7 gave somewhat lower values for the temperature than the thermocouple used for the experiments of Figure 8. It should also be noted that a 50 K uncertainty at 1200 K represents only a 4% error in absolute temperature.

Discussion

The experiments described in this paper were designed to characterize the properties and reactions of both B_2O_3 and B_2O_2 directly deposited on a boron surface. Both boron oxides have been shown to play a role in the reaction of solid boron with O_2. Although XPS spectra of boron surfaces oxidized with O_2 showed characteristics consistent with a small coverage of B_2O_3, it was not clear whether the spectra might not also be consistent with B_2O_2 on the surface. Our results show that the two oxides can be distinguished with XPS. The B(1s) chemical shift is ≈4.5 eV in B_2O_2 where the boron has a formal oxidation number of +2; in B_2O_3 the chemical shift is 5.8 eV and the boron oxidation number is +3. This suggests that at least for boron oxides, the B(1s) chemical shift is roughly proportional to the oxidation number. The distinctly different B(1s) binding energy in B_2O_2 and B_2O_3 is also consistent with the distinctly different bonding in the isolated molecules. B_2O_2 has a linear O=B—B=O structure while B_2O_3 has a V-shaped O=B—O—B=O structure.[10]

We assume that the B_2O_2 layer deposited on the boron surface has the properties of solid B_2O_2. While solid B_2O_3 is well-known, far less work has been done on solid B_2O_2 which is also referred to as boron monoxide or $(BO)_x(s)$. Gal'chenko et al. have reviewed all reported boron-oxygen compounds.[5] Two methods of preparing solid $(BO)_x$ have been described. The first method[6,7] involves dehydrating $B_2(OH)_4$ by heating to ≈500 K. We have used the second method[8-14] which involves condensing the $B_2O_2(g)$ which results from reduction of B_2O_3. The solid thus obtained is generally described as an amber glassy material while the first method yields a white solid. While a few chemical properties of $(BO)_x(s)$ have been described, the material's physical and structural properties do not appear to have been established. However, most evidence indicates that there are both B—B and B=O bonds and possible structures have been proposed.[5] The XPS results we present in Figure 5, which indicate that B_2O_2 disproportionates to boron and B_2O_3 at temperatures between 600 and 800 K, are consistent with a report by Nicholls[14] that condensed B_2O_2 turns black when heated above 600 K which Nicholls attributed to the same disproportionation reaction that we observe.

Since the disproportionation of B_2O_2 into B_2O_3 and boron appears to be completed by 800 K, the desorption of $B_2O_2(g)$ at temperatures above 1050 K indicates that B_2O_2 forms again either before or at the desorption temperature. The annealing experiments of Figure 5 indicate that the oxide is not irreversibly converted back into B_2O_2 prior to oxide desorption. Rather, the surface oxide appears to remain in the form of B_2O_3 throughout the desorption process. The same behavior was observed when the oxide was initially deposited as B_2O_3. Annealing experiments have the disadvantage of revealing only irreversible changes with temperature rather than the actual state of the surface at a given temperature.

The isotopic distribution of the B_2O_3 and B_2O_2 desorption products following the initial deposition of isotopically pure $^{10}B_2O_3$ reveals extensive isotopic exchange between the boron film and the oxide layer. Our experiments provide no information on the temperature at which this exchange begins. The completeness of the exchange implies that it takes place well below the onset of desorption at ≈1050 K. It also seems reasonable to suppose that it takes place above the melting point of B_2O_3 at 723 K. One possibility is that the exchange simply occurs between the molten B_2O_3 layer and the substrate and that the exchange is complete by the time the B_2O_3 chemically reacts to produce B_2O_2 which then immediately desorbs. Another possibility is that the following equilibrium is established well below the desorption temperature:

$$2B_2O_3 + 2B \rightleftharpoons 3B_2O_2$$

where both the forward and reverse reactions are fast. Below the B_2O_2 desorption temperature the equilibrium would greatly favor the reactants. This would explain why only B_2O_3 is detected on the surface with XPS after annealing to above 800 K in the experiments of Figures 4 and 5. As the B_2O_2 is removed from the equilibrium mixture through desorption, the equilibrium would shift to the left to give more B_2O_2 until all of the oxide had desorbed. We would then have to assume that the

desorption temperature of B_2O_3 is coincidently about the same as that of B_2O_2 to account for the small amount of B_2O_3 desorption observed.

In our previous study of the reactions of $^{10}B_2O_3$ with the (111) surface of β-rhombohedral boron we observed results quite similar to those reported here. There we suggested that the B_2O_3 reacted with the boron substrate to make B_6O, a material which is produced through this reaction but under rather different conditions than used in our experiments. The reaction

$$^{10}B_2O_3 + 16B \rightarrow 3B_6O$$

would clearly yield an isotopic composition of the product fairly close to that of the boron substrate. Mass spectroscopic studies[16] show that when heated, B_6O decomposes in vacuum to liberate primarily B_2O_2(g) along with smaller amounts of B_2O_3. The B(1s) binding energy in B_6O, in which boron has a formal oxidation number of only +1/3, is unlikely to be resolvable from the B(1s) peak of elemental boron. Although the extensive isotopic exchange we observe does not allow a unique reaction mechanism to be determined, it does reveal that some complex surface chemical processes are occurring prior to oxide desorption.

Conclusions

Through a direct deposition of B_2O_3 and B_2O_2 on a boron surface, we have established that these two boron oxides can be distinguished with XPS. Heating a boron surface on which either B_2O_3 or B_2O_2 has been deposited at room temperature leads to the desorption of B_2O_2(g) at temperatures of 1050–1200 K. The reason the deposited B_2O_2 gives the same results as deposited B_2O_3 at high temperatures is that B_2O_2 disproportionates between 600 and 800 K to B_2O_3 and B. These results then imply that the desorption of B_2O_2 following oxidation through exposure to O_2 is completely consistent with B_2O_3 being the only oxide formed on the surface from the reaction of O_2 with boron.

Acknowledgment. This work was supported by a grant (AFOSR-92-J-0179) from the Air Force Office of Scientific Research.